

Computer Assisted and Contour Detection in Medical Imaging Using Fuzzy Logic

Hmadri nath moulick¹, Joyjit Patra², Arun kanti Manna³

^{1&2}(Asst.Prof, C.S.E. dept.,Aryabhatta Institute Of Engineering And Management, Durgapur, W.B)

³(Asst.Prof, C.S.E. dept.,Modern Institute Of Engineering And Technology,Bandel,Hooghly W.B)

ABSTRACT:- *Soft computing (e.g. fuzzy logic, neural network, genetic algorithms) has proved to yield promising results in digital image processing and understanding when missing, ambiguous or distorted data is available [2][3]. For biomedical image analysis, archiving and retrieval, the great structural information may be successfully approached by using methods of soft computing. Moreover, symbolic calculus (e.g. predicate logic, semantic nets, frames, scripts) may be used for knowledge representation, thus merging the expert's domain into a decision support system. This paper describes the use of fuzzy logic and semantic knowledge for edge detection and segmentation of magnetic resonance (MR) images of brain. Promising results show the superiority of this knowledge-based approach over best traditional techniques in terms of segmentation errors. The proposed methodology can be successfully used for model-driven in the domain of MRI.*

The information in medical imaging is structured on multiple layers: semantic and numerical. Several algorithms for shape and color detection which can be used for numerical analysis are presented in this paper. Semantic information can be extracted from numerical information using fuzzyfication. For a correct image interpretation and a diagnosis formulation several of the objects features (shape, color, orientation and spatial relations between different objects) are required. Based on these algorithms and features, this paper proposes a system that can mimic the thinking of a human medic. The system consists of a fuzzyfication engine that converts the numerical data into linguistic data. A medical knowledge database is implemented and a fuzzy inference engine is used. The medical image will be analyzed by numerical algorithms for any signs of disorder. In addition a search feature will be implemented for searching in medical databases for similar cases to confirm or infirm the diagnosis if one is discovered.

KEYWORDS: - *medical imaging, artificial vision, smoothing, registration, segmentation.*

I. INTRODUCTION

Medical images are one of the basic diagnosis tools. They hold a lot of information about the patient and the disease. The image can be divided in two image data layers: the upper or semantic data layer which is used by the medic and the lower or numerical layer which is used by computers [1], [2]. Between these two worlds there is a big gap because humans use associations and semantic variables to interpret the image, while computers use mathematical formulas and exact numbers to analyze the image. Objects from the image can be considered as a group of adjacent and similar pixels, and by analyzing the properties of this group the properties of the object can be found. The numeric values and the semantic values are not independent at all, a close dependency can be observed. This paper proposes an automated medical image interpretation using numerical and semantic variables as well. The conversion from numerical to semantic values will be done using fuzzyfication. First the image is analyzed using numerical methods for shape, color and size. These values will be fuzzyficated, and using an inference engine and a medical knowledge database to interpret the values. The found values are sent to query the internet and the medical image databases to find similar cases to support or infirm the diagnosis found by the inference engine and the knowledge database.

II. MEDICAL IMAGING

Medical images carry information on low (numerical) level and high (semantic) level [1,2]. Data from this level can be divided in metadata which are indirectly connected to the image and content data. The metadata contains information about the hospital, the medic's general observations, and information about associated diseases and about the image physical properties. The content level is rich in features, characteristic and salient objects. These objects can represent organs as a set of geometrical structures, or their internal structure. The signs or the absence of some signs belongs too to the content level. On the low level or numerical level the mathematical values of the image can be found. These numbers represent borders, colors, size and location. However numerical values are more precise than semantic values, for a human being a simple number does not mean much, humans associate the numbers to a semantic value. By converting these numerical values to a high level semantic value the computer can correctly interpret the image and formulate a diagnosis, and can

somehow mimic the thinking process of a human which is based on association rather than on complex numerical formulas. A computer to properly investigate and interpret the image, it needs some numerical algorithms to investigate the low level data from the image. Several low level data detection algorithms are presented in this section.

III. SHAPE DETECTION

One of the major features of the object is its contour's shape. The detection of the border can be made using fuzzy or numeric methods. As an example of applying a fuzzy technique, the paper [3] describes the detection of the shape of the lateral ventricles of the CSF (cerebrospinal fluid) in a 3D image. The whole CSF consists of the lateral ventricles, the third and fourth ventricles and other regions. In 3D images the unit is the voxel, which is the equivalent of a 2D pixel. The image is evaluated using 2 primary steps: the lowest value of the CSF is set as the intensity threshold Th_{low} and an edge voxel is obtained Va . The image is segmented in subimages having 26 voxels per subimage. The Va must satisfy two criteria: the Va must not be included in the edge region or the brain, and the intensity of the Va must be higher than Th_{low} . The method automatically finds a representative line, which is followed and then dilated until the line contains the whole lateral ventricle. To evaluate the direction of the line three features: medialness, insideness and curvature are defined. Medialness evaluates the position of the representative line in the CSF. It can be described as:

$$x_M(s, \vec{d}) = \int \epsilon(s + t\vec{d}) dt \quad \dots\dots\dots(1)$$

Where s is the end of the representative line, d is the tracking direction and $\square\square(p)$ is the Euclidian distance from a point P to the background. Insideness evaluates the position of the representative line in the inter-cranial region, it must be in the center of that region.

$$x_I(s, \vec{d}) = \int \lambda(s + t\vec{d}) dt \quad \dots\dots\dots(2)$$

where $\square\square(p)$ is the Euclidian distance from p to the region contour. The curvature x_c evaluates the shape of the representative line using conventional image processing techniques [4]. A fuzzy if then rule set is defined to find the most suitable direction: IF medialness is high AND insideness is high, AND curvature is low, THEN the degree of the directions is high. From a starting point, the method traces the line in the direction with the highest fuzzy degree. The lateral ventricles are segmented by applying: for each CSF voxel a perpendicular is calculated to the representative line, each voxel that has its perpendicular only in the CSF are classified as class A voxels, the other class B. The voxels from the representative line and the class B voxels are set as ultimate eroded points. With UEP's and the watershed segmentation algorithm the region with the representative line is decompressed. Another approach for image interpretation can be made using RBF (radial basis function) neural network algorithm [5]. The used RBF neural network has a three layer architecture using input, hidden and output layers. The architecture can be seen in the Figure 1.

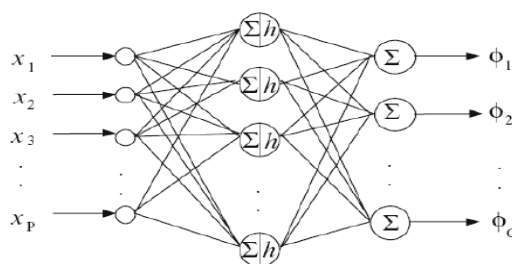


Fig. 1. The proposed algorithm for the organ and the abnormality detection

The input layer can be described as:

$$u_i = x_i \quad (i = 1, 2, \dots, p) \quad \dots\dots\dots(3)$$

Where u_i is the output x_i is the input of the neurons and p is the total number of the input variables. In the hidden layer the output is expressed as:

$$k_j = \exp\left(-z_j^2\right) \quad (j = 1, 2, \dots, q) \quad \dots\dots\dots(4)$$

Where z_j is estimated with the regression analysis for the training data.

$$z_j = a_0 + a_1 d_j; \quad d_j = \|u - c\| \quad \dots\dots\dots(5)$$

Where a_j ($j \in \{0, 1\}$) are the regression coefficients and d_j are the distances between the training data (u) and center of the neuron (c). The output of the output layer is described as:

$$\phi_i(x) = \sum_{j=1}^g w_j h_j(u) \dots\dots\dots(6)$$

Where w_j are the weights of the neural network and g is the total number of the neurons from the output layer. The weights are estimated using multiple regression analysis. In this type of structure, the structural parameters like means and variances of the radial basis functions are determined from the training data without any other computation. Another algorithm uses object windows to isolate the object from the rest of the image [6]. Firstly the image is scanned using the Peak and Valley algorithm following the Hilbert curve. The equations of the Peak and Valley algorithm are the following:

$$p'(i+j) = \min(p(i-1), p(i+k))$$

$$\text{if } p(i+j) < p(i-1) \text{ and } p(i+j) < p(i+k) \dots\dots\dots(7)$$

$$p'(i+j) = \max(p(i-1), p(i+k))$$

$$\text{if } p(i+j) > p(i-1) \text{ and } p(i+j) > p(i+k) \dots\dots\dots(8)$$

$$p'(i+j) = p(i+j) \text{ in other situations.}$$

$$\forall j = 0, 1, 2, \dots, k-1 \dots\dots\dots(9)$$

Where $p(i)$ is the original intensity value of the pixel i . $p'(i)$ is the new intensity of the pixel. Equation (7) represents a valley value of a k number pixel group, equation (8) represents the peak pixels and (9) is when non of (7) or (8) applies. The next step is to find all local peak and valley values and substitute the intensity values of pixels with the interpolation values. A local adaptive threshold is applied with the Otsu algorithm to found a global threshold to classify the pixels. Found objects are set to white and the rest of the image to black. All distinct objects are labeled and their features are computed using min/max values, orientation, area and column/row coordinates. The objects are shown and separated from the rest of the image using object windows. By comparing the found features from the object window with the known features of the searched object, a candidate object is chosen. If none found, the thresholds are modified and a new search is done, on the found object a morphological filtering is used to smoothen out the object.

IV. FUZZY ICONIC LEVEL

A. Fuzzy Image Processing: A two-dimensional (2D) fuzzy image $F/M, N$ is a 2D real function $f(x, y)$ defined on each pixel coordinate (x, y) so that $0 \leq x < M, 0 \leq y < N$ and $0 \leq f(x, y) \leq 1$. The fuzzy image reflects some specific properties, e.g. brightness, edginess and texture, that are defined by the membership function $f(x, y)$. The membership function has often a triangular form. As alternatives, fuzzy logic uses specific nonlinear functions, such as Z, S, or U [14]. So, a fuzzy image is the projection of a digital image by a membership function. If more fuzzy images are assigned to one single 2D image, then the fuzzy image is represented by a 3D image whose third dimension is defined by the number of fuzzy images:

$$f(x, y) : I_{M,N} \rightarrow F I'_{M \times N} ; f(x, y) \in [0, 1]; i \in \{1, 2, \dots, K\}, \dots\dots\dots(10)$$

where K indicates the number of possessed properties, as above. Figure 2 shows a typical fuzzy image processing procedure.

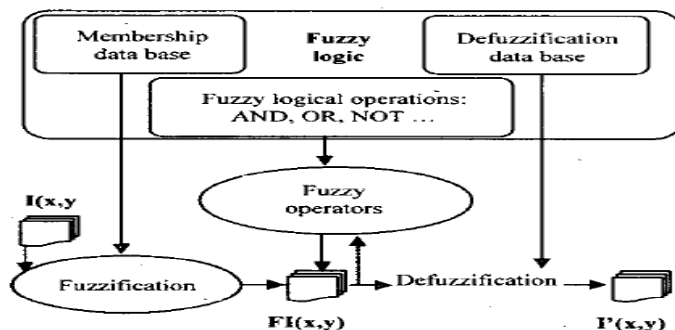


Figure 2. Block diagram of typical fuzzy image processing

B. A Fuzzy Knowledge-Based Contour Detection Technique: The objective of OUF contour-based segmentation procedure 'is the detection of fuzzy contour of objects. The term fuzzy does not refer to the shape of contours but to their representation mechanism. The elements of our sets are image points. The sets are labeled with contour names (e.g. backgroundskin). Each set member is assigned a value on the interval [0, 1]

representing its grade of membership for a contour. We refer to fuzzy sets in function notation with image point vectors as arguments.

$$f_{\text{contour name}} : [0 \dots N]^2 \rightarrow [0, 1], \quad 0 \leq f_{\text{contour name}} \leq 1 \dots (11)$$

contours are represented in frames, which comprise parametrical and relational knowledge for each desired contour. Fuzzy sets for each contour are calculated collecting evidence by means of well defined operationalizations of assertions in the frames. We first describe some methods for operationalization of knowledge, and then present the frame representation of contours together with an example.

(a) Gradient: Evidence for a contour is its high gray value gradient in input images. So with the assertion "The BackgroundUSkin contour has a high gradient in the p image" (Figure 2) and $|g_p(x)|$ is the magnitude of the gradient of p , normalized to the interval $[0, 1]$, we follow that

$$f_{\text{background/skin}}(x) \leq |g_p(x)| \dots (12)$$

We use "5" as the conjunction of the above assertion and all other assertions about this specific contour should be used to define the fuzzy set for the contour. A conjunction is expressed by a **minimum** operation in fuzzy set formalism. Of course, the initial value of each fuzzy set value should be one, as no assertion can increase fuzzy values.

(b) Direction: As long as we are dealing with convex objects, we may employ valuable information using direction of the gradient. We define a centre c_p of our images and a direction vector d , depending on X .

$$c_p = \frac{\sum p(x)}{\sum 1}, \quad d(x) = c_p - x \dots (13)$$

The assertion "The direction of the p gradient is inside for the Background&kin contour" can be operationalized with unit Vectors g'_i and d'_o

$$f_{\text{background/skin}}(x) \leq N_{\text{pos}}(g'_p(x) \cdot d'_p(x)) \dots (14)$$

N_{pos} is a normalization function that maps all negative values to 0 and normalizes all positive values linearly to the interval $[0, 1]$. The constraint function is proportional to the angle between the gradient and d'_i . If the direction is outside, d'_o is used with opposite sign.

C. Relations: In addition to contour detection based on gradient values and directions, we may also use relations among contours. With an assertion like "The backgroundhkin contour is outside the skinhone contour" we may constrain $f_{\text{background/skin}}$ by saying that $f_{\text{background/skin}}(x)$ must not exceed the largest value of $f_{\text{skin/bone}}$ along a line between x and c_p

$$f_{\text{background/skin}}(x) \leq N_d \max_{0 \leq \lambda \leq 1} (f_{\text{skin/bone}}(x + \lambda d_p(x))) \dots (15)$$

N_d is again a normalization factor, which is determined for each d to map values on $[0, 1]$. If the maximum-term is very low, there is a low plausibility for the d contour inside point x and therefore a low plausibility for x being outside of

$f_{\text{skin/bone}}$. Similarly, inside can be defined as

$$f_{\text{bone/brain}}(x) \leq N_d \max_{\lambda=0} (f_{\text{skin/bone}}(x + \lambda d_p(x))) \dots (16)$$

V. THE INTERPRETATION PLATFORM

The proposed platform can be divided in several layers. The top layer is the input layer which can be a live feed from a transducer or a stationary image from a database or mobile storage device. On the second layer the image is filtered for noise reduction, to eliminate as much inference as it can be eliminated without affecting the quality of the image. Like this the image is prepared for the low level image feature extraction using similar algorithms as presented in section 2. On the third layer where the numerical scanning takes place, the image is scanned for relevant objects. If contours are found they are scanned for size, color and relative position to each other. The raw data obtained is in form of number arrays. These number arrays can be considered as sub-images. To be analyzed, they are fuzzyficated, and prepared for the next processing layer. For each sub-image an array of semantic variables are created and stored in a buffer. The fourth layer is the semantic operation level where the fuzzyfication and fuzzy inference is located [9], [10]. The inference engine takes each semantic array and correlates them with data found in the medical knowledge database. The medical knowledge database stores

information about the organs: their shape,color pattern,spatial position and illnesses;about other formations like artifacts which can be disguised as organs or anomalies but they are just gas or fluids;symptoms and the diagnosis of illnesses [11], [12].The inference engine retrieves information from the database and compares with the data from the fuzzyfication engine.The found results are then sent to a display unit and if a network connection is available then to the internet to query medical databases for similar cases,as a safety self supervising feature to confirm the diagnosis or infirm it if necessary.In Figure 3 the flowchart of the system is presented:

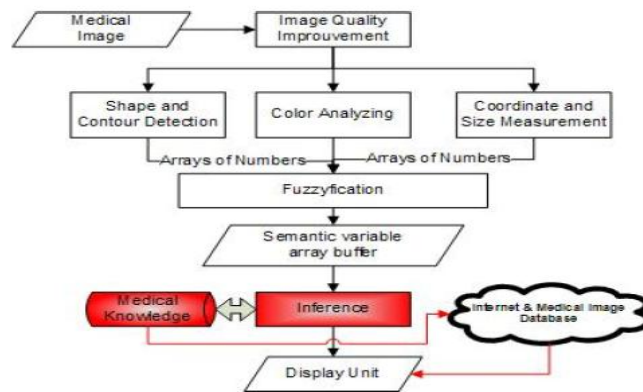


Figure 3.

The shape and color detection will be made using similar methods to those that were presented in the previous section.The colors, which in grayscale images are shades of grey from white to black,represent solid and fluid objects.The black objects have a higher absorbance ratio then the white objects.This means that black objects are soft objects and the white spots represent solid objects like bones or calcifications.First the image is segmented in n*n sized sub-image.Each sub-image is analyzed separately.For each sub-image a mean histogram is calculated.For this each value of each pixel must be obtained and a mathematical mean value calculated.The pixel number in one sub-image must not be high,not to compromise the main histogram of the image.The different shades of gray represent different consistency and this can be used as one of the features after which the organ is identified.Using fuzzyfication for each subimage a semantic value can be assigned.The fuzzyfication of the histogram is made using trapezoidal membership function.Like this we can ignore some slight shade differences.The histogram of a pixel has a value from 0 to 255. The value zero is obtained if the investigated subimage is black, and the 255 value is obtained if the subimage is white. In Figure 4 several objects are shown having different colors:

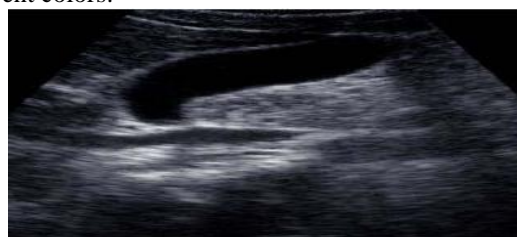


Fig. 4. Gall bladder and bowel gas

The long big black object is the gall bladder; the horizontal grayish object under the gall bladder is bowel gas which is an artifact.This means it is not an object of interest.The color can be fuzzyficated using trapezoidal membership functions,presented in Figure 5

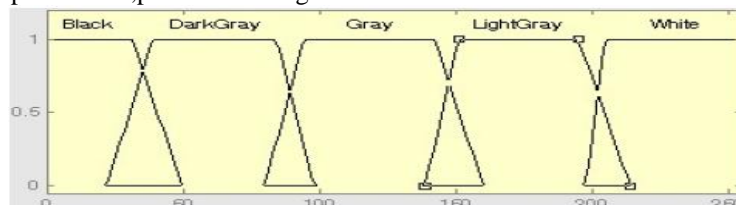


Figure 5. The grayscale histogram membership functions

This allows us easy access to the features of the fuzzification engine. Also the mean histogram of the subimage can be used as input value .
 Examples of the suggested rules for the consistency of the object found are:

if Black is High then object is Fluid
if DarkGray is High then object is Gas
if White is High then object is Reflective

In our case the white spot is the intestine. It must be known how the organ appears in the image from different scanning position. Because the scanning wave in ultrasound has limited depth, some soft tissue can appear as reflective tissue. The size and shape detection and fuzzyfication is still a work in progress. For the size determination the selected region's actual pixel number must be obtained, and the most important, the pixel size must be obtained, in other words the system must know how big the surface is represented by the pixel. The actual resolution of the image is important because if the image has a bigger resolution the pixel covers a smaller area from the object. The relative position of the objects must be taken in consideration. One object can be inside of another object, or on the left or the right side, or one on top of another. Using these relative positions the system can decide if the second object is a potential pathological formation or an image artifact. The medical knowledge database contains symptoms signs and features of the organs, artifacts, pathological formations and their relative positions to each other and the diagnosis in semantic variables. The logical structure of the medical knowledge database is similar to a look-up table. This confers high speed in searching for a diagnosis and the possibility for fast actualization. The fuzzy inference engine is the hearth of this system. Its functional logic is simple but effective. It collects data from the fuzzyfication engine and searches in the database for correlations. The inference engine takes each array of semantic variables and searches for similar data sets in the medical knowledge database. If similarities are found between values then the object represented by the array can be identified. Like this, artifacts can be eliminated which appear in the image as some sort of pathological object. The second step is to make a correlation between objects. If some spatial or other dependencies are found and it is known that the second object, in many cases smaller the organ, is an anomaly of the organ, we can assume that a pathological object of the organ is found. Like this a diagnosis can be formed. Because the medical knowledge database is structured as a look-up table, the values can be easily verified. If they are not found they can be introduced in the database. In this case the architecture of the knowledge database can be easily modified and expanded. The new values are just simply attached to the end of the vectors from which the look-up table is composed. This table can be an n dimensional permitting a simpler value correlation. The new element of this system is that while other systems searches for well defined signs and only for one type of anomaly, this system takes in count all the signs from the image and tries to identify where and what is the anomaly, not just looking for one kind of pathological object. For a higher precision the system will be equipped with a searching module. This serves for searching medical databases for similar cases. It is important to rule out the possibility of a false diagnosis, which in some cases can be fatal for the patient.

VI. CONTOUR DETECTION

Image segmentation is **one** of the most important steps leading to the analysis of digital images, its main goal being to divide an image into (disjoint) parts that have a strong correlation with objects or areas of the real world. Among the low-level segmentation methods, there are two different approaches. The first involves **region-based segmentation**: classification by thresholding, looking for sets of attributes, region growing, division and merging. The second approach involves **contour-based segmentation** (looking for local discontinuities): derivatives operators, active contours (*snakes*), and mathematical morphology. These two groups of methods solve a dual problem, in the **sense** that each region can be represented by its closed boundary, and each closed boundary describes a region. The region adjacency graph is an usual example of this duality. These methods often lead to missing edge pieces (gaps) or ambiguities if no domain specific knowledge about the expected contours is incorporated. Because of the different natures of the various edge and region based techniques, they may be expected to give somewhat different results in information and consequently the segmentation itself is not unique. Contours in biomedical imaging have a fuzzy nature due to grayness ambiguity, arising from the inhomogeneity of contrast of identical anatomical objects; (ii) spatial ambiguity, coming from variations in size, shape, position and pathological variability; (iii) partial volume effects, i.e. the image of two tissues in one voxel, (and pixel). Therefore, exact decisions about the location of contour points are in principle impossible, but "best estimate" decisions can be made, as physicians do when interactively defining the outlines of anatomical structures (regions of interest-ROI).

VII. ROBUST CONTOUR DETECTION

As traditional edge detectors applied to fuzzy contours yield unwanted gaps, we approached this task as a search of **an** optimal path between two known points of the contour that optimizes a cost function, by using a breadth-first graph search strategy. Four initial points acting both as starting point and end point of different contour segments were chosen. The result is a closed border made by four contour segments. searches for initial

points in the four directions d_4 separated, and selects the points having the maximal product of $Ipp(x)$ and **fuzzy** contour values for each.

A. Cost Function: Each image pixel are attached four features:

- (i) $\Phi(x) = \arctan(g_x(x)/g_y(x))$, gradient direction;
- (ii) $I_g(x)$, gradient magnitude;
- (iii) $QC(x) = \lfloor \frac{g(x)}{255} \rfloor + \lfloor \frac{g(x)}{255} \rfloor \cdot d \pmod n$;
- (iv) $L_{nr.umomu}(x)$, fuzzy contour values. The transfer **cost function** for each possible contour point is defined as

$$C(x, x') = (C_1(x, x') + w C_2(x, x')) f(x'), \dots\dots\dots(17)$$

x and x' being two neighbouring points with x' a candidate successor of x and w a weight. The terms of (8) are as follows:

$$C_1(x, x') = \Delta_g(x, x') = |g(x') - g(x)| + |g(x') - g(x_{end})| \dots\dots\dots(18)$$

with x_{end} the predefined contour end point. This term assures local continuity when referring to gradient values.

$$C_2(x, x') = \Delta_\alpha(x, x') = [|\Phi_C(x) - \alpha(x, x')| + |\Phi_C(x') - \alpha(x, x')|] / 2, \dots\dots\dots(19)$$

with α denoting the direction of $(x-x')$ line. $C_1(x)$ is upper bounded by a threshold value, θ , whose exceeding sets C_2 to infinity. Both terms capture small global variations of gradient and assure early quit of paths with high costs. Moreover, this cost function favors smooth contours and small deviations of the path direction α from the contour direction $\Phi_C(x)$. The term $f(x')$ is defined according to formula

$$f(x') = 2 - f_{contourname}(x') \dots\dots\dots(20)$$

and it comes from the knowledge-based contour detection phase.

VIII. RESULT

We used experimentally the following values for tuning the cost function computation: $w=0.70$ in (8), $\theta = 70$. $n=30$ nodes were used for graph search procedure. Results of the contour detection for the images in Figure 9 are displayed in Figures 6 and 9, respectively. In order to assess the effectiveness of fuzzy contour detection, a comparison with two traditional edge detection methods (Sobel and Canny operators) have been shown. In our study only very little knowledge about the desired contour was used. Figure 9 presents a p -weighted image of a brain with tumor. One can observe its low contrast, which is a severe impediment for traditional edge detection techniques. In comparison with the very popular Canny filter our method yields superior results concerning the accuracy of edge detection. Figure 10 shows segmentation results obtained by using model knowledge and semantic networks. Thus, **ventricles** from T₁-image (Figure ~2b), the **tumor** from "Tumor?-image and the imagistic fuzzy set **inside(bone)** with contours superposed were obtained after a short processing time. In general, the use of iconic fuzzy sets partially overcomes the problems of contrast normalization, histogram equalization, filtering a.s.o, which must be used with traditional techniques when we are faced with low variable contrast and noisy images.

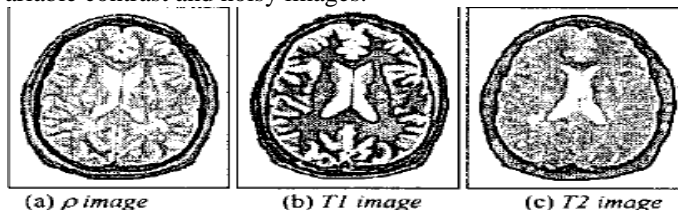


Figure 6. p , T1 and T₂ images of an axial MM section

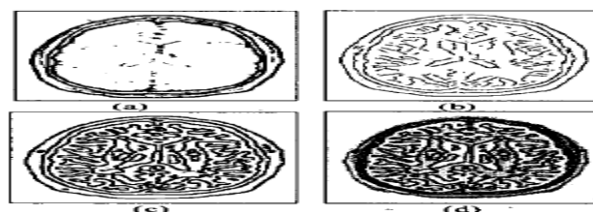


Figure 7. p image: Sobel (a); Canny (b); **fuzzy contour** (c); (c)

$$C_2(x, x') = \Delta_\alpha(x, x') = [|\Phi_C(x) - \alpha(x, x')| + |\Phi_C(x') - \alpha(x, x')|] / 2, \dots\dots\dots(19)$$

with a denoting the direction of $(x-x')$ line. $C_c(x)$ is upper bounded by a threshold value, 0 , whose exceeding sets C_2 to

infinity. Both terms capture small global variations of gradient and assure early quit of paths with high costs. Moreover, this cost function favors smooth contours and small deviations of the path direction α from the contour direction $\Phi_c(x)$. The term $f(x')$ is defined according to formula

$$f(x') = 2 - f_{\text{contourname}}(x') \dots \dots \dots (20)$$

and it comes from the knowledge-based contour detection phase. We used experimentally the following values for tuning the cost function computation: $w=4.70$ in (8), $\theta = 70^\circ$. $n=30$ nodes were used for graph search procedure. Results of the contour detection for the images in Figure 9 are displayed in Figures 6 and 9, respectively. In order to assess the effectiveness of fuzzy contour detection, a comparison with two traditional edge detection methods (Sobel and Canny operators) have been shown. In our study only very little knowledge about the desired contour was used. Figure 9 presents a p-weighted image of a brain with tumor. One can observe its low contrast, which is a severe impediment for traditional edge detection techniques. In comparison with the very popular Canny filter our method yields superior results concerning the accuracy of edge detection. Figure 10 shows segmentation results obtained by using model knowledge and semantic networks. Thus, ventricles from T₁-image (Figure ~2b), the tumor from "Tumor?-image and the imagistic fuzzy set inside(bone) with contours superposed were obtained after a short processing time. In general, the use of iconic fuzzy sets partially overcomes the problems of contrast normalization, histogram equalization, filtering a.s.o, which must be used with traditional techniques when we are faced with low variable contrast and noisy images.

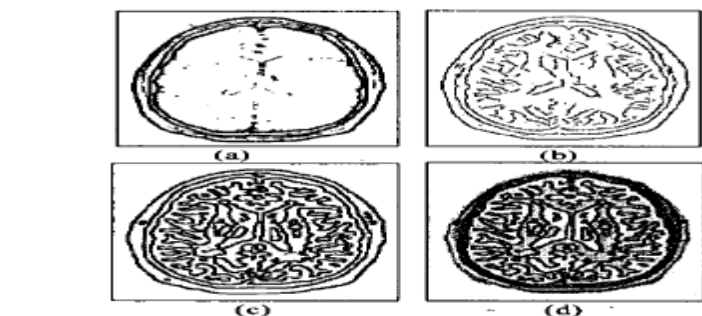
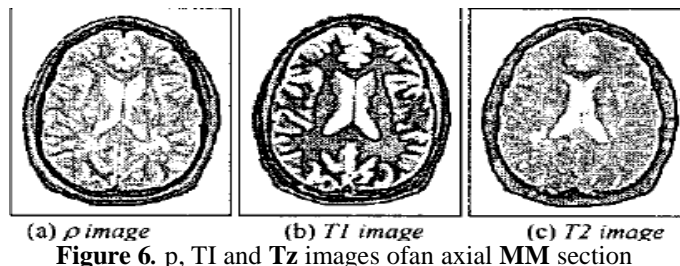


Figure 7. p image: Sobel (a); Canny (b); fuzzy contour (c); (d)

IX. CONCLUSION

Now-a-days medical imagistics is still a vast realm, where crisp and fuzzy methods are in use. The proposed system tries to mimic the thinking process of the medic. The modularity of the system gives flexibility for the system, and can be adapted very easily for different situations. Using the trapezoidal membership functions the fuzzyfication process can be easily adapted for improvement; thresholds can be set or modified. This is important when the image is blurred or the histogram is affected by noise. The position must not be exact, because a crisp value of 340x20 Cartesian position of the object means very little for a human in contrast with the upper left corner semantic variable. The knowledge base and inference engine is robust in this architecture and can be easily maintained. As future researches we take into account the fuzzyfication of the shape, the relative spatial position and the development of a module for Evidence Based Medicine. Another issue that must be solved is the color pattern detection and association. In some cases like the kidney, the major contour of the organ is gray, but inside the organ there are physiological black triangles, the medullas and the beginning of the urethra and the renal pelvis are physiologically white. In the knowledge database must be

implemented each feature of the organ, how they appear as normal organs, and how they appear as pathological objects. Our paper describes the **use** of **fuzzy** logic and semantic knowledge for contour-based segmentation of magnetic resonance images of brain. Promising results show the superiority of this knowledge-based approach over best traditional and other **fuzzy** techniques in terms of segmentation errors [4][6][7][10]. The proposed concept can be successfully **used** for model-driven image analysis in the domain of MRI. This method also has the potential for a data-driven approach. Measurements of features of fuzzy images can be represented in a semantic net as fuzzy assertions [12]. Definition of a hyperrelational structure allows us to express the dependency of relations on facts (e.g. "CSL is inside bone only if there is no fracture"). Possible faults (pathologies) can be **further** incorporated by using information from other sources (neurological studies) as fuzzy assertions. Besides, contour shape models may be used in the graph search algorithm.

X. ACKNOWLEDGMENT

The authors are thankful to Mr. Saikat Maity & Dr. Chandan Koner for the support to develop this document.

REFERENCES

- [1]. Richard Chbeir, and Franck Favetta, : A Global Description of Medical Imaging With High Precision, IEEE TRANSACTIONS ON SYSTEMS, MAN, AND CYBERNETICS—PART B: CYBERNETICS, VOL. 33, NO. 5, OCTOBER 2003, Digital Object Identifier 10.1109/TSMCB.2003.816911
- [2]. Mueen, R. Zainuddin and M. Sapiyan Baba: Automatic Multilevel Medical Image Annotation and Retrieval; Journal of Digital Imaging, Vol 21, No 3 (September), 2008; pp 290Y2
- [3]. Syoji Kobashi, Tomokazu Takae, Yuri T. Kitamura, Yukata Hata, Toshio Yanagida: Fuzzy medical image processing for segmenting the lateral ventricles from mr images, 0-7803-6725-110 IEEE.
- [4]. J. C. Russ, The Image Processing Handbook, 3rd ed., Boca Ration, FL, CRC, 1998.
- [5]. Masahiro Nakagawa • Tadashi Kondo • Tsuyosi Kudo Shoichiro Takao • Junji Ueno: Three-dimensional medical image recognition of cancer of the liver by a revised radial basis function (RBF) neural network algorithm, Artif Life Robotics (2009) 14:118–122 © ISAROB 2009, DOI 10.1007/s10015-009-0640-y.
- [6]. Nualsawat Hiransakolwong: Automated Liver Detection in Ultrasound Images, W.-K. Leow et al. (Eds.): CIVR 2005, LNCS3568, pp. 619–628, 2005. © Springer-Verlag Berlin Heidelberg 2005.
- [7]. Hui-Yu Huang, Yung-Sheng Chen and Wen-Hsing Hsu: Integrating Color, Texture, and Spatial Features for Image Interpretation. K. Aizawa, Y. Nakamura, and S. Satoh (Eds.): PCM 2004, LNCS 3331, pp. 327–334, 2004. c, Springer-Verlag Berlin Heidelberg 2004.
- [8]. Na Wang, Guo-Yu Wang: Shape Descriptor with Morphology Method for Color-based Tracking. International Journal of Automation and Computing 04(1), January 2007, 101-108, DOI: 10.1007/s11633-007-0101-9.
- [9]. The MathWorks, Inc. User's Guide Version 2: Image Processing Toolbox For Use with MATLAB®, September 2000 Revised for Version 2.2.2 (Release 12) (Online only).
- [10]. The MathWorks, Inc. User's Guide Version 2: Fuzzy Logic Toolbox User's Guide For Use with MATLAB®, July 2002 Online only Revised for Version 2.1.2 (Release 13).
- [11]. Günter Schmidt, MD: Thieme Clinical Companions Ultrasound; c 2007 Georg Thieme Verlag, Rüdigerstrasse 14, 70469 Stuttgart, Germany, 10-ISBN 3-13-142711-6;
- [12]. Jovitas Skucas, MD: Advanced Imaging of the Abdomen, Springer-Verlag London Limited 2006, ISBN-10: 1-85233-992-6 e-ISBN 1-84628-169-5.
- [13]. Ballard D. and Brown C. Computer Vision, Englewood Cliffs, NJ, Prentice-Hall, 1982. Costin H. and Rotariu Cr. "Tremor assessment by means of handscript analysis and fuzzy logic", Biomedical Soft Computing and Human Sciences, Japan, Vol. 7, No. 1, Dubois D., Prade H., Yager R. (eds.): Readings in Fuzzy Sets for Intelligent Systems, Morgan Kaufmann Publ., 1993.
- [14]. Fletcher-Heath J.M., et al. "Automatic segmentation of non-enhancing brain tumors in MR images", *Artificial Intelligence in Medicine*, 21, 2001, pp. 43-63. Foster M.A. and Hutchinson J.M. (eds.). *Practical NMR Imaging*, IRL Press, Oxford, 1987. Laurent M.C., et al. "Application of a fuzzy method for the segmentation of renal angiograms", *Proc. of EUFIT'97, 1997*, pp. 2355-2359.
- [15]. Jendrysik F., Eichfeld H., Graumann R. "Fuzzy segmentation method applied to the extraction of kidney boundaries in medical images", *Proc. of EUFIT'97, 1997*, pp. 2360-2364.
- [16]. Nilsson N.J. *Principles of Artificial Intelligence*, Tioga Publishing Co., Palo Alto, Ca., 1980.
- [17]. Rich E. *Artificial Intelligence*, McGraw Hill, 1983. [10] Singh A., Goldgof D., Terzopoulos D. (eds.) *Deformable Models in Medical Image Analysis*, IEEE Computer Society Press, Los Alamitos, California 1998.
- [18]. Sonka M., Hlavac V., Boyle R. *Image Processing, Analysis and Machine Vision (2d ed.)*, PWS Publishing 1999.
- [19]. Sowa J.F. (ed.). *Principles of semantic Network. Explorations in the Representation of Knowledge*, Morgan Kaufmann Publ., Inc., 1991.
- [20]. Teodorescu H.N., Kandel A., Jain L.C. (eds.): *Fuzzy and Neuro-Fuzzy Systems in Medicine*, CRC Press, 1999. Wang L.-X.. *A Course in Fuzzy systems and Control*, Prentice-Hall international, Inc., 1997.